Available online at www.sciencedirect.com
ScienceDirect
Journal of Nuclear Materials 367–370 (2007) 677–684
journal of nuclear materials
www.elsevier.com/locate/jnucmat

Swelling of SiC at intermediate and high irradiation temperatures

L.L. Snead *, Y. Katoh, S. Connery

Metals and Ceramic Division, Oak Ridge National Laboratory, P.O. Box 2008, MS-6138, Oak Ridge, TN 37831-6140, USA

Abstract

This paper presents results from a neutron irradiation campaign on CVD SiC carried out in the High Flux Isotope Reactor. Materials were irradiated in a range of temperature from 200 to 1500 °C and from a fraction of a dpa to ~6 dpa. Data on swelling and room temperature thermal conductivity are presented. The swelling behavior below ~800 °C agrees well with the literature values. Data in the range of 1000–1600 °C indicates that swelling increases as the dose is increased from 2 dpa to 6 dpa, at higher-swelling with increasing irradiation temperature. Any peak in void swelling apparently occurs at irradiation temperature >1500 °C (>0.6T_m). In the 1100–1200 °C temperature range, volumetric swelling is apparently at a minimum though increases from ~0.2% to ~0.4% as dose increases from ~2 dpa to ~6 dpa. The maximum swelling was found to be ~1.5% at the maximum dose and temperature of this study, ~6 dpa and ~1500 °C. Room temperature thermal conductivity data over the entire temperature range are presented and a direct correlation between the thermal defect resistance and swelling is seen for materials irradiated at temperature less than 800 °C. Above 1000 °C the correlation between swelling and thermal defect resistance breaks down indicating a changing microstructure at high temperature to a microstructure less effective at scattering phonons on a swelling-normalized basis.

1. Introduction

The neutron-induced swelling and degradation in thermal conductivity of silicon carbide (SiC) has been well studied for low and intermediate temperatures (~20–1000 °C). Originally this material was investigated in support of nuclear fuel coating [1–9] and more recently for various nuclear applications such as structural SiC composites [10–23]. Before proceeding, it is important to distinguish neutron-induced effects in high-purity materials, such as single crystal and most forms of chemically vapor deposited (CVD) SiC, with those of lower purity forms such as hot pressed, sintered, liquid phase converted, or polymer-derived SiC. It is well understood that the presence of significant impurity levels in these materials leads to unstable behavior under neutron irradiation [12,15,24,25] as compared to stoichiometric materials, which exhibit remarkable radiation tolerance. This paper presents new and previously published data only for stoichiometric, near theoretical density, SiC.

Previous work describing the dimensional swelling and thermal conductivity behavior of SiC for irradiation temperatures in excess of 1000 °C is

* Corresponding author. Tel.: +1 865 574 9942; fax: +1 865 241 3650.
E-mail address: SneadLL@ornl.gov (L.L. Snead).

0022-3115/$ - see front matter © 2007 Elsevier B.V. All rights reserved.
doi:10.1016/j.jnucmat.2007.03.097

quite limited [1,2,4,18], and as some authors note, suffers from uncertainty as to the irradiation temperature. The purpose of this paper is to accurately determine the swelling behavior and thermal conductivity reduction for fully dense stoichiometric SiC at doses to ~6 displacements per atom (dpa), for irradiation temperatures up to 1600 °C.

2. Experimental

Materials evaluated in this paper are CVD SiC manufactured by Rohm & Haas and single crystal 6H–SiC produced by Cree, Inc. Manufacturer information for the CVD SiC describes a face centered cubic β-SiC of density 3.21 g/cc (theoretical is 3.217) and grain size of 5 μm. The chemical purity measurements by gas discharge mass spectroscopy and neutron activation yields >99.9995% SiC (metals basis). It is likely that gaseous elements such as nitrogen exist in the ppm range. The single crystal material is a true single crystal α-type 6H structure with purity exceeding that of the CVD SiC with a reported doping level of 4×10^{17} nitrogen atoms/cm^3.

Two fission reactor irradiation campaigns on SiC were carried out in the core region of the High Flux Isotope Reactor (HFIR) at the Oak Ridge National Laboratory. The peak thermal and fast neutron flux of the core is $\sim 2.5 \times 10^{19}$ (thermal) and 9×10^{18} n/m^2 s ($E > 0.1$ MeV). The irradiations are described as follows.

2.1. Rabbit capsule irradiation

In the first campaign a series of small capsules (rabbit capsules) were irradiated in the hydraulic tube of the HFIR. In these capsules 6 mm diameter samples of variable thickness (typically 3–8 mm) were loaded inside a graphite holder and welded under an inert gas inside the aluminum outer capsule. The sample thickness was selected based on an assumed post-irradiation thermal diffusivity to give a relevant rise time according to ASTM 1461 [26]. The sample irradiation temperatures were varied by a combination of variable gap thickness between the holder and the inner diameter of the aluminum capsule, and the type of capsule gas used (helium, neon, or argon). The irradiation temperature of the rabbit capsules was measured by isochronal annealing of SiC temperature monitors while observing the thermal conductivity change. Application of such a technique is described elsewhere and has been shown to be accurate up to 800 °C and for irradiation doses as low as 0.001 dpa [27]. The irradiation temperature and neutron fluence for these capsules ranged from 200 to 800 °C and 0.01 to 4×10^{25} n/m^2 ($E > 0.1$ MeV), respectively. Throughout this paper an equivalence of 1×10^{25} n/m^2 ($E > 0.1$ MeV) = 1 dpa is assumed.

2.2. Fixed-core irradiation

The second irradiation campaign includes data from the first two in a series of three fixed-core capsules irradiated in HFIR in the temperature range of 900–1600 °C. The peak fast neutron fluences for the two fixed-core capsules discussed here are ~2 and $\sim 6 \times 10^{25}$ n/m^2 ($E > 0.1$ MeV, ~2 and 6 dpa, respectively). Each capsule contained 10 subcapsules, individually containing many specimens. The specimens were nominally 5.8 mm in diameter with varied thicknesses. A subset of subcapsules from the 6 dpa capsule had 3 mm thick samples appropriate for thermal conductivity measurement. The samples were loaded in contact with a high-purity graphite holder and the capsule environment was high-purity argon. On both ends of the subcapsules cylinder were threaded graphite caps that included eight cylindrical wells each containing a melt-wire. The melt-wires were pure materials or binary alloys specifically blended to achieve a select melting temperature. For a given subcapsule the design temperature was achieved by varying the gas gap between the outside of the sample holder and the inner diameter of the capsule containment. The maximum subcapsule irradiation temperature was then determined by viewing the melt-wires following irradiation. The melt-wires were arrayed to compensate for either an overestimation or underestimation of the true temperature of the subcapsules. Typical intervals between melt-wires was ~20 and 40 °C. A temporal variation in temperature within a subcapsule is expected due to the radiation-induced dimensional change of the Poco AXF-5Q holder (thus changing the gap between the sample holder and capsule containment). No change in temperature due to variation in reactor power is expected due to the exceptionally steady power history of the HFIR reactor during the irradiations. The error bars associated with the temperature estimation herein are a combination of the melt-wire intervals and the changing gas gap.

2.3. Measurement techniques

Sample densities were measured using the density gradient column technique [28] utilizing a mixture of tetrabromethane and methylene iodide and certified, calibrated floats. A typical gradient column ranged approximately 0.1 g/cc over ~1 m of column height. The experimental uncertainty in density measurement was estimated to be 0.003%. The density shown for the highest dose fixed-core capsule is made up of two to three CVD SiC samples from each subcapsule. The density of samples from individual subcapsules was identical in many cases and therefore indistinguishable as plotted. All samples were soaked in hydrofluoric acid for 30 min and rinsed in alcohol prior to immersion to remove any surface oxide on the SiC. However, for all but the highest irradiation temperature, no surface reaction was observed and no sample mass loss was detected following irradiation or acid bath.

The room temperature thermal conductivity (K) was calculated using the measured thermal diffusivity (α), measured density (ρ), and the assumed specific heat (C_p) of 667 J/kg K as follows: $K = \alpha\rho C_p$. The thermal diffusivity of every specimen was measured before and after irradiation using an Anter Systems Flashline 5000 with a solid-state detector. The conversion from diffusivity to conductivity assumed a specific heat unchanged by irradiation. This common assumption is known to be valid for graphite [29] though has not been thoroughly demonstrated for ceramics.

3. Results and discussion

The irradiation-induced microstructural evolution of CVD SiC is fairly well understood and has been reviewed recently by Katoh [30]. The contribution of the defects themselves to the swelling in SiC is less well understood, especially at elevated temperatures. Below several hundred degrees Celsius the observable microstructure of neutron irradiated SiC is described as containing 'black dots' which are most likely tiny clusters of self-interstitial atoms in various indeterminate configurations. For irradiation temperatures less than about 150 °C, accumulation of strain due to the self-interstitial atoms leads to a critical level above which the crystal becomes amorphous. This has been shown for both self-ion irradiation and under fast neutron irradiation [31–33]. As shown by Katoh [32], the swelling at 50 °C under self-ion irradiation increases linearly with dose until amorphization occurs. The swelling of neutron-amorphized SiC has been reported to be 10.8% for 70 °C irradiation [33]. However, there is evidence that the density of amorphous SiC will depend on the conditions of irradiation (dose, temperature, etc.) [34].

For temperatures above the critical amorphization temperature the swelling saturates after a few dpa, with a steady decrease in the saturation swelling level with increasing irradiation temperature. At very high doses [35] and/or higher temperatures such as 900–1400 °C [4,18,36], Frank faulted loops of interstitial type become the dominant defects observed by transmission electron microscopy. Under silicon ion irradiation at 1400 °C, the development of Frank loops into dislocation networks through unfaulting reactions at high doses is reported [36]. The volume associated with dislocation loops in irradiated SiC has been estimated to be smaller than 0.1% [37,38].

At temperatures where vacancies are sufficiently mobile, vacancy clusters can be formed. Three-dimensional cavities (or voids) are the only vacancy clusters known to commonly develop in irradiated SiC. The lowest temperature at which void formation was observed under neutron irradiation is 1250 °C [39]. Senor reported the lack of void production after neutron irradiation to 0.9×10^{25} n/m^2 at 1100 °C, though voids were observed after subsequent annealing at 1500 °C for 1 h [18]. Under silicon ion irradiation, voids start to form at 1000 °C at very low density and become major contributors to swelling at irradiation conditions of 1400 °C at >10 dpa [37]. The work by Senor implies limited vacancy mobility prohibits observable void production at 1100 °C for a neutron dose up to 0.9 dpa [18]. However, positron annihilation and electron paramagnetic resonance studies have shown that the silicon vacancy in cubic SiC becomes mobile at 800–900 °C [40,41]. Therefore, it would not be surprising for void swelling to take place at as low as ~1000 °C at high doses, particularly for low damage rate irradiations.

For the materials of this study, the non-irradiated density of CVD SiC at 20 °C was 3.2101 g/cc and that of single crystal 3.2107 g/cc. The density of the non-irradiated samples was quite uniform within the samples studied, typically within the 0.003% experimental error. Fig. 1 gives data for swelling of both the CVD and single crystal SiC materials irradiated in the fixed-core capsule as a function of irradiation temperature along with

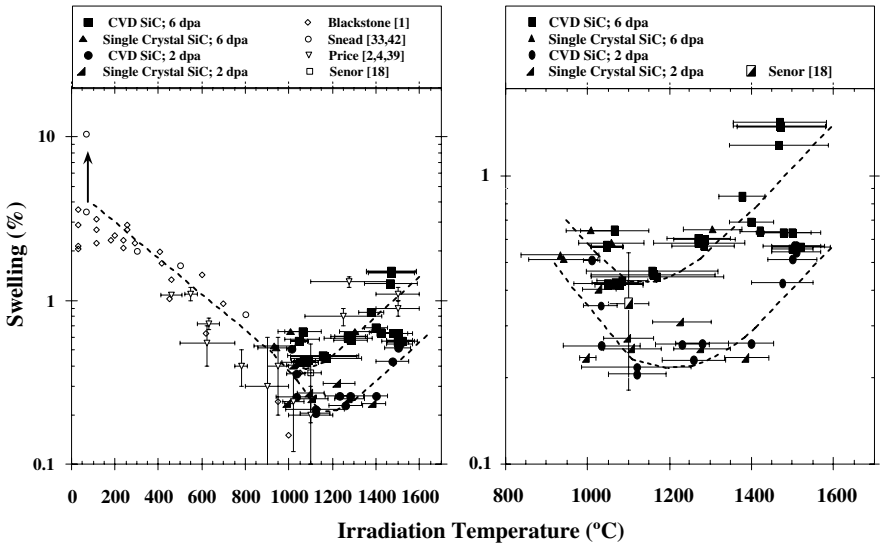

Fig. 1. Volumetric swelling of SiC as a function of neutron irradiation temperature.

historical data on stoichiometric, near full density CVD SiC. Data on swelling from the rabbit capsule irradiations are not included here because the majority of samples were irradiated to fluences less than saturation swelling levels. Error bars on temperature have been included for all the high-temperature data from this experiment, and in some cases those of the literature data. Error bars on swelling have also been included, though the measurement error for density in some cases is such that the error bars are not resolvable. It is noted that the CVD SiC data of Blackstone and Voice [1] is excluded due to the presence of free silicon and low density of that material. In the 1100–1200 °C temperature range, volumetric swelling is apparently at a minimum though increases from ~0.2% to ~0.4% as dose increases from ~2 dpa to ~6 dpa. Clearly the swelling in this temperature range has not saturated by 2 dpa. Above this minimum in swelling the data indicates a continual swelling increase to the maximum temperature of ~1600 °C. This finding is somewhat surprising given the apparent mobility of the silicon vacancy above 1000 °C found experimentally in cubic SiC (The CVD SiC of this study is highly faulted FCC.) [40,41].

Fig. 1 includes historical data for swelling above 1000 °C [2,4,18,33,39,42]. Specifically, Senor [18] reports swelling for the same type of CVD SiC irradiated in this study, also irradiated in a water moderated fission reactor (the ATR). His maximum dose, irradiation temperature and swelling data were ~1 dpa, ~1100 ± 30 °C, and 0.36 ± 0.02%. The irradiation temperature quoted in Senor's work was a best estimate though the author also provides an absolute bound for his experiment of 800–1200 °C. The maximum swelling in the Senor work (0.36 ± 0.02% at ~1 dpa) is somewhat higher than the ~0.25% swelling at 2 dpa, ~1100 °C of the present work. This is seen from the rightmost figure of Fig. 1. Also seen on the figure (left) is the high-temperature swelling of Price [2,4,39]. The Price data, which are in the dose range of about 4–8 dpa, are in fair agreement with the measured swelling of this study. The highest swelling material (~1250 °C, ~6 and 10 dpa) shows the largest discrepancy, though if the true irradiation temperature were at the rightmost part of the error bar, this data would also be more consistent with the present work. It is also noted that the Price material may have had some excess silicon leading to higher-swelling as compared to stoichiometric material. There does not appear to be a difference in swelling between the highly faulted FCC β-SiC and the single crystal HCP α-SiC in the present study.

As mentioned earlier, the microstructural evolution of irradiated SiC is fairly well understood, at least for temperatures up to ~1100 °C. The swelling near the critical amorphization temperature (~150 °C) is classically described as the differential strain between the single interstitial, or tiny interstitial clusters, and the contraction of immobile vacancies. As the temperature increases above the critical amorphization temperature the number of defects surviving the cascade are reduced and the mobility

of both silicon and carbon interstitials becomes significant. For temperature approaching ~1000 °C microstructural studies have noted the presence of both Frank loops and tiny voids indicating limited mobility of vacancies. The apparent increase in swelling in the 1000–1500 °C range, and the assumed production of voids, is interesting considering the maximum irradiation temperature of this study is ~0.60 of the melting temperature (T_m) for SiC. It is noted that the melting temperature is somewhat variable in the literature. Here we have assumed the value of Olesinski [43] of 2545 °C where stoichiometric SiC transforms into C + liquid phase. This value of $0.65T_m$ is high when viewed in comparison to FCC metal systems where void swelling typically begins at $\sim 0.35T_m$, goes through a maximum value, and decreases to nil swelling by $\sim 0.55T_m$. (It is noted that the melting and dissociation temperature of SiC are somewhat variable in the literature. Even considering this variability the previous statement is still accurate.) If, as the swelling data seems to indicate, the voids in SiC are continuing to grow in SiC irradiated to 1600 °C the energies for diffusion of one or both the Si and C vacancy must be quite high, as are the binding energies for clustered vacancies. This has been shown through theoretical work in the literature [44–47]. However, it is noted that the defect energetics obtained from that body of work, and in particular those of the Si and C vacancy, SiC vary widely. Perhaps the work of Bockstedte [45] following an ab initio approach, is the most accurate yielding a ground state migration energy for Si and C vacancies of 3.5 and 3.4 eV, respectively. It was also noted by Bockstedte [45] that the charge state of the vacancy will effect the migration energy. Specifically the carbon vacancy in the +1 and +2 charge state increases from 3.5 to 4.1 and 5.2 eV, respectively and that of silicon in the +1 charge state increases from 3.4 to 3.6 eV. Several papers discuss the vacancy and vacancy cluster mobility measured experimentally. The silicon monovacancy has been shown to be mobile below 1000 °C. Using photoluminescence Sorman [48] and Wagner [49] find the Si vacancy disappearing above 750 °C. Using electron spin resonance the carbon vacancy is shown to anneal above 1400 °C [50]. Using isochronal annealing and positron lifetime analysis Lam [46] has shown a carbon–silicon vacancy complex to dissociate above ~1500 °C for the same 6H single crystal materials studied here.

Room temperature thermal conductivity for CVD SiC is given in Fig. 2 for the 6×10^{25} n/m^2 ($E > 0.1$ MeV) capsule as a function of irradiation temperature. Also included in Fig. 2 are literature data on Rohm–Haas CVD silicon carbide irradiated in this dose range for irradiation temperatures <800 °C. The degradation in thermal conductivity, for $T < 800$ °C is certainly due to phonon scattering from small vacancy clusters in the crystal and can be considered saturation values [13].

The non-irradiated room temperature thermal conductivity in the current study is 327 ± 25 (one standard deviation) W/m K. It is noted that significant plate-to-plate and intra-plate thermal conductivity variability exists for this particular grade of CVD SiC [13,23]. For irradiation temperature above about 1200 °C the room temperature thermal conductivity (Fig. 2) is seen to dramatically increase. This is attributed to the lack of the small vacancy clusters at this temperature, having been annihilated by migrating interstitials or formed into larger defects that are less effective at scattering phonons. The phonon scattering at such high temperature is now likely dominated by larger defects less effective in scattering phonons on a volumetric basis. For the highest irradiation temperature of this study (1468 ± 120 °C) the as-irradiated room temperature thermal conductivity is ~111 W/m K, or about 34% of the non-irradiated value.

Based on the previous work of Price [4] on the high-temperature swelling behavior CVD SiC it is expected that the current data presented in Fig. 2 do not represent saturation values in thermal conductivity. In his work, swelling continued to

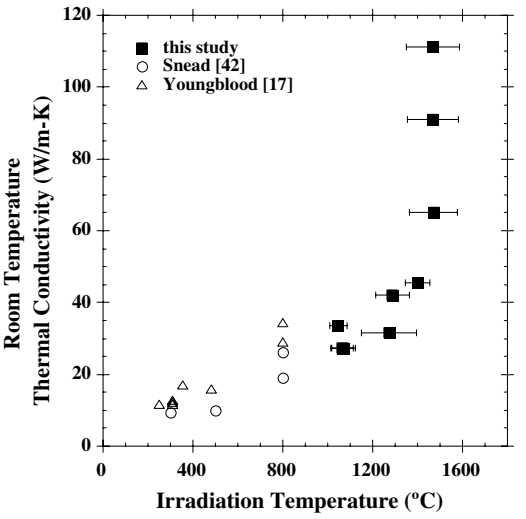

Fig. 2. Room temperature thermal conductivity of SiC irradiated in the 4–8 dpa range as a function of irradiation temperature.

increase in the 1250–1500 °C irradiation temperature range to about 1 dpa. It is most likely that the defects dominating the as-irradiated thermal conductivity at temperatures >1000 °C are a combination of Frank loops and voids. In particular, voids are expected to continue to evolve in the high-temperature range causing increased swelling and reduction in thermal conductivity. Recent work by Senor [18] indicated a continued degradation in room temperature thermal conductivity for Rohm and Haas CVD SiC in the 0.5–1 dpa range at 1100 °C. No data exists above 10 dpa at these elevated temperatures. No conclusion can be drawn from this study relative to the continued degradation in thermal conductivity with increased dose since thermal conductivity measurements have not been completed at both doses. However, it is noted that a single sample from the lower dose capsule (~2 dpa, ~1503 ± 75 °C) yielded a value of 90.5 W/m K, very similar to the 6 dpa, 1470 ± 114 °C sample (Fig. 2).

The nature of the microstructural development in the transition from the intermediate to high irradiation temperature range is fairly well understood. Moreover, a program of TEM and positron annihilation planned for the materials discussed here should demonstrate quantitatively the defect evolution. However, it can be shown that there is a clear change in the defects controlling the thermal conductivity through the simple analysis of 'thermal defect resistance' [51]. The thermal defect resistance is defined as the difference in the reciprocal of the irradiated and non-irradiated thermal conductivity ($1/K_{rd} = 1/K_{irr} - 1/K_{non-irr}$). This term can be related directly to the defect type and concentration present in irradiated ceramics [51]. Fig. 3 gives a compilation of data from this study for both thermal conductivity and thermal defect resistance as a function of swelling. Data from previous work are not considered. As seen from the plot, as swelling increases the thermal conductivity rapidly degrades from its non-irradiated value of 327 ± 25 W/m K to a saturation value of about 10 W/m K. However, by plotting the same data as thermal defect resistance leads to a clear linear relationship with swelling for irradiation temperatures where swelling is attributed to interstitial strain, in this case for material irradiated from 200 to 800 °C. This data is the bulk of the data from the rabbit capsule irradiations. At these temperatures, vacancies are considered to have very limited mobility and form at most very tiny clusters. The implication here is

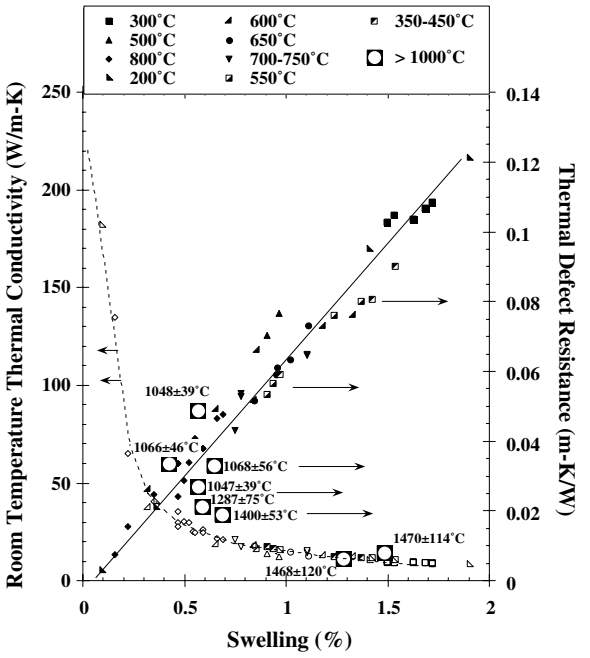

Fig. 3. Room temperature thermal conductivity and thermal defect resistance as a function of swelling of SiC. Irradiations at greater than 1000 °C are 6 dpa data. Open symbols related to those in legend refer to thermal conductivity. Legend symbols refer to thermal defect resistance.

that the small vacancies or vacancy complexes dominating phonon scattering are correlated with the interstitial strain causing swelling at $T_{irr} < 800$ °C. Fig. 4 shows a weak beam dark field TEM image of CVD SiC irradiated at 300 °C (left) and 800 °C (right) to approximately 7 dpa in a related study [30]. Both microstructures reveal the presence of what is generally referred to as black dots, though the 800 °C microstructure has a loop diameter of ~3 nm, or three times that of the 300 °C irradiated microstructure. Additionally the loop density has decreased by about an order of magnitude as these defect coarsen. It is interesting to note that the correlation between swelling and thermal defect resistance is independent of the coarsening microstructure shown in Fig. 4. It is further noted that the swelling-thermal defect resistance relationship can serve to estimate the thermal conductivity reduction of SiC by the simple measurement of swelling.

The correlation between swelling and thermal defect resistance does not hold as the irradiation temperature increases above 1100 °C. On Fig. 3 the largest symbols refer to the 6 dpa CVD SiC irradiated in the fixed-core capsules. On the plot the

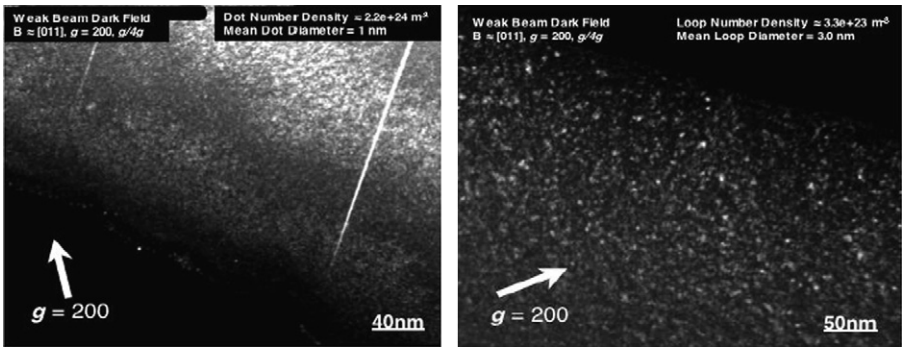

Fig. 4. TEM image of CVD SiC irradiated to ~7 dpa at 300 °C (left) and 800 °C (right). Arrow represents the reflection (*g*) vector [30].

irradiation temperature is plotted to the right of the symbol. For materials irradiated in the 1015–1100 °C range the thermal defect resistance roughly fall within the scatter band of the thermal defect resistance data. However, as the irradiation temperature is increased above ~1300 °C the thermal defect resistance clearly falls below the 'correlation line' with the material irradiated at higher temperature exhibiting much lower phonon scattering. The fact that the 1015–1100 °C irradiated materials are consistent with the correlation line may be fortuitous. However, the reduced thermal defect resistance for the higher-swelling, higher-temperature irradiated materials clearly indicate that the defects dominating thermal conductivity are much less effective on a volume normalized basis in scattering phonons. The assertion that voids would be less effective phonon scattering center is not new, having been theoretically explained by Klemens and Pedraza [52].

4. Conclusions

Data have been presented for swelling and thermal conductivity of high-purity CVD SiC over the irradiation temperature range of 200–1600 °C. Below about 800 °C data on swelling is consistent with literature data. A robust set of data has been presented for irradiation above 1000 °C indicating that swelling continues to increase as the irradiation dose is increased from 2 to 6 dpa. In the 1100–1200 °C temperature range, volumetric swelling is apparently at a minimum though increases from ~0.2% to ~0.4% as dose increases from ~2 dpa to ~6 dpa. While no conclusion can be made with this data relative to saturation in swelling in the 1100–1200 °C temperature range, it is likely that the swelling at this irradiation temperature is due to a combination of tiny clusters and Frank loops. However, it is also possible that part of the swelling at this temperature is due to voids. If this is the case the material will continue to swell for fluences greater than that studied here. A detailed microstructural examination is currently underway and will follow in a companion paper. For temperature greater than 1200 °C the swelling of SiC appears to increase with increasing irradiation temperature up to ~1500 °C with the level of swelling scaling with the dose for the 2 and 6 dpa irradiations. The swelling appears to be increasing even for the highest temperature irradiation achieving greater than 1.5% swelling at ~1470 °C.

A direct correlation between the thermal defect resistance and swelling of SiC in the irradiation temperature range of 200–800 °C has been shown. This dependence appears to be independent of irradiation temperature indicating that the defects controlling both swelling and thermal conductivity are the same independent of the temperature-driven coarsening of the observable SiC microstructure. Evaluation of the thermal conductivity on this basis also will be useful in predicting the thermal conductivity of SiC simply on the basis of swelling. For irradiation temperatures >1200 °C the correlation between thermal defect resistance and swelling breaks down indicating that the small vacancy cluster evolve to large structures (such as voids) that are less effective phonon scattering centers per unit volume.

Acknowledgements

The authors thanks Marie Williams for her assistance with thermal diffusivity experiments and Stas Gulobov for enlightening discussion. Additionally the authors are thankful to Katey Lenox, Dennis Heatherly, and Bob Sitterson for their efforts in

carrying out the irradiation and post-irradiation examinations. This research was sponsored by the Office of Fusion Energy Sciences, US Department of Energy under contract DE-AC05-00OR22725 with UT-Battelle, LLC. Additional support was provided by the Department of Energy through a Nuclear Energy Research Initiative grant.

References

[1] R. Blackstone, E.H. Voice, J. Nucl. Mater. 39 (1971) 319.
[2] R.J. Price, J. Nucl. Mater. 33 (1969) 17.
[3] R. Price, Nucl. Technol. 35 (1977) 320.
[4] R.J. Price, J. Nucl. Mater. 48 (1973) 47.
[5] W. Primak, L.H. Fuchs, P.P. Day, Phys. Rev. 103 (1956) 1184.
[6] M. Balarin, Phys. Status Solidi 11 (1965) K67.
[7] N.F. Pravdyuk et al. (Eds.), Properties of Reactor Materials and the Effects of Radiation Damage Proceedings, Butterworth, London, 1962.
[8] R.P. Thorne, V.C. Howard, B. Hope, Proc. Br. Ceram. Soc. 7 (1967).
[9] R. Stevens, Philos. Mag. 25 (1972) 523.
[10] J.C. Corelli et al., J. Am. Ceram. Soc. 66 (1983) 529.
[11] H. Miyazaki et al., J. Nucl. Sci. Technol. 29 (1992) 656.
[12] R. Matthews, J. Nucl. Mater. 51 (1974) 203.
[13] L.L. Snead, J. Nucl. Mater. 329–333 (2004) 524.
[14] L.L. Snead, J. Nucl. Mater. 326 (2004) 114.
[15] G.W. Hollenberg et al., J. Nucl. Mater. 219 (1995) 70.
[16] D.J. Senor et al., Fus. Technol. 30 (1996) 943.
[17] G.E. Youngblood, D.J. Senor, R.H. Jones, Fusion Reactor Materials Semiannual Report DOE/ER-0313/33, 2002, p. 27.
[18] D.J. Senor et al., J. Nucl. Mater. 317 (2003) 145.
[19] W. Dienst et al., J. Nucl. Mater. 174 (1990) 102.
[20] T. Iseki et al., J. Nucl. Mater. 170 (1990) 95.
[21] C.W. Lee, F.J. Pineau, J.C. Corelli, J. Nucl. Mater. 108&109 (1982) 678.
[22] H. Suzuki, T. Iseki, M. Ito, J. Nucl. Mater. 48 (1973) 247.
[23] G.E. Youngblood, D.J. Senor, R.H. Jones, J. Nucl. Mater. 329–333 (2004) 507.
[24] L.L. Snead, T. Hinoki, Y. Katoh, Fusion Reactor Materials Semiannual Report DOE/ER-0313/33, 2002, p. 49.
[25] G. Newsome et al., J. Nucl. Mater., submitted for publication.
[26] ASTM. Standard Test Method for Thermal Diffusivity by the Flash Method E 1461-01.
[27] L.L. Snead, A.M. Williams, A.L. Qualls, in: M.L. Grossbeck (Ed.), The Effects of Radiation on Materials: 21st International Symposium, ASTM STP 1447, 2003.
[28] ASTM, D1505-85, Standard Test Method for Density of Plastics by Density Gradient Technique, 1985.
[29] J.W.H. SimmonsRadiation Damage in Graphite, vol. 102, Pergamon, 1965.
[30] Y. Katoh et al., J. Nucl. Mater., in press.
[31] L.L. Snead, S.J. Zinkle, in: I.M. Robertson, G.S. Was, L.W. Hobbs, T.D.d.l. Rubia (Eds.), Microstructure Evolution During Irradiation, vol. 439, Materials Research Society, Pittsburgh, 1997, p. 595.
[32] Y. Katoh, H. Kishimoto, A. Kohyama, J. Nucl. Mater. 307–311 (2002) 1221.
[33] L.L. Snead et al., Nucl. Instrum. and Meth. B 141 (1998) 123.
[34] L.L. Snead, S.J. Zinkle, Nucl. Instrum. and Meth. B 191 (2002) 497.
[35] T. Yano et al., J. Nucl. Mater. 253 (1998) 78.
[36] S. Kondo et al., J. Fus. Sci. Technol. 2 (2003) 181.
[37] Y. Katoh et al., in: International Conference on Fusion Reactor Materials-12, Santa Barbara, CA, USA, J. Nucl. Mater., submitted for publication.
[38] S. Kondo, in: International Conference on Fusion Reactor Materials 12, 2005, Santa Barbara, CA, USA, J. Nucl. Mater., submitted for publication.
[39] R.J. Price, J. Nucl. Mater. 46 (1973) 268.
[40] H. Itoh, N. Hayakawa, I. Nashiyama, J. Appl. Phys. 66 (1989) 4529.
[41] A. Kawasuso, H. Itoh, D. Cha, Appl. Phys. A – Mater. Sci. Process. 67 (1998) 209.
[42] L.L. Snead et al., J. Nucl. Mater. 307–311 (2002) 1141.
[43] R.W. Olesinski, G.J. Abbaschian, Bull. Alloy Phase Diagrams 5 (1984) 486.
[44] H.C. Huang et al., Modell. Simul. Mater. Sci. Eng. 3 (1995) 615.
[45] M. Bockstedte, A. Mattausch, O. Pankratov, Phys. Rev. B 68 (2003) 205201.
[46] C.H. Lam et al., Mater. Res. Soc. Symp. Proc. 792 (2004) R3.19.1.
[47] J. Li, L. Porter, S. Yip, J. Nucl. Mater. 255 (1998) 139.
[48] E. Sorman et al., Phys. Rev. B 61 (2000) 2613.
[49] M. Wagner et al., Phys. Rev. B 66 (2002) 144214.
[50] L.A.D. Balona, J.H.N. Lousber, J. Phys. C: Solid State Phys. 3 (1970).
[51] L.L. Snead, S.J. Zinkle, D.P. White, J. Nucl. Mater. 340 (2005) 187.
[52] P.G. Klemens, D.F. Pedraza, Carbon 32 (1994) 735.